

Spatial Damped Anomaly Persistence of the sea-ice edge as a benchmark for dynamical forecast systems

Bimochan Niraula¹ and Helge Goessling²

¹Alfred-Wegener-Institut Helmholtz-Zentrum für Polar- und Meeresforschung

²Alfred Wegener Institute Helmholtz Centre for Polar and Marine Research

November 22, 2022

Abstract

Accelerated loss of the sea-ice cover and increased human activities in the Arctic emphasize the need for skillful prediction of sea-ice conditions at sub-seasonal to seasonal (S2S) time scales. To assess the quality of predictions, dynamical forecast systems can be benchmarked against reference forecasts based on present and past observations of the ice edge. However, the simplest types of reference forecasts –persistence of the present state and climatology– do not exploit the observations optimally and thus lead to an overestimation of forecast skill. For spatial objects such as the ice-edge location, the development of damped-persistence forecasts that combine persistence and climatology in a meaningful way poses a challenge. We have developed a probabilistic reference forecast method that combines the climatologically derived probability of ice presence with initial anomalies of the ice-edge location, both derived from satellite sea-ice concentration data. No other observations, such as sea-surface temperature or sea-ice thickness, are used. We have tested and optimized the method based on minimization of the Spatial Probability Score. The resulting Spatial Damped Anomaly Persistence forecasts clearly outperform both simple persistence and climatology at sub-seasonal timescales. The benchmark is thus about as skilful as the best-performing dynamical forecast system in the S2S database. Despite using only sea-ice concentration observations, the method provides a challenging benchmark to assess the added value of dynamical forecast systems.

1 **Spatial Damped Anomaly Persistence of the sea-ice**
2 **edge as a benchmark for dynamical forecast systems**

3 **Bimochan Niraula¹, Helge F. Goessling¹**

4 ¹Alfred-Wegener-Institut Helmholtz-Zentrum für Polar- und Meeresforschung

5 **Key Points:**

- 6 • We have developed a new method that combines climatological sea-ice probabili-
7 ty and initial-state anomaly to forecast sea-ice presence.
8 • Ice-edge forecasts derived from this method can outperform climatological bench-
9 marks at lead times of up to 2 months.
10 • Spatial damped anomaly persistence forecasts have a higher predictive skill than
11 most models from the sub-seasonal to seasonal database.

Corresponding author: Bimochan Niraula, bimochan.niraula@awi.de

Abstract

Accelerated loss of the sea-ice cover and increased human activities in the Arctic emphasize the need for skillful prediction of sea-ice conditions at sub-seasonal to seasonal (S2S) time scales. To assess the quality of predictions, dynamical forecast systems can be benchmarked against reference forecasts based on present and past observations of the ice edge. However, the simplest types of reference forecasts – persistence of the present state and climatology – do not exploit the observations optimally and thus lead to an overestimation of forecast skill. For spatial objects such as the ice-edge location, the development of damped-persistence forecasts that combine persistence and climatology in a meaningful way poses a challenge. We have developed a probabilistic reference forecast method that combines the climatologically derived probability of ice presence with initial anomalies of the ice-edge location, both derived from satellite sea-ice concentration data. No other observations, such as sea-surface temperature or sea-ice thickness, are used. We have tested and optimized the method based on minimization of the Spatial Probability Score. The resulting Spatial Damped Anomaly Persistence forecasts clearly outperform both simple persistence and climatology at sub-seasonal timescales. The benchmark is thus about as skillful as the best-performing dynamical forecast system in the S2S database. Despite using only sea-ice concentration observations, the method provides a challenging benchmark to assess the added value of dynamical forecast systems.

Plain Language Summary

The Arctic is becoming more ice free and seeing more human activities, which means it is important to have reliable forecasts of sea-ice conditions weeks to months ahead. The accuracy of a forecast system is typically compared against reference forecasts based on present and past observations of the ice-edge location. However, the most widely used references either simply maintain the current state or consider states at the same time of the year during previous years. Such simple benchmarks can lead to an overestimation of how “skillful” a forecast system is considered. In the case of sea-ice edge, creating a better reference forecast combining both historical and current observation information can be challenging. We have addressed this challenge and developed a method that combines the historical probability of ice presence with the current location of the ice edge. The new method clearly outperforms the simpler methods and remains slightly better than historical-based forecasts even 2 months ahead. Despite using only observed sea-ice concentration data (like the simpler benchmarks), the new benchmark is about as good as the best modern model-based forecast system. The method therefore provides a good reference to study how well the latest forecast systems are actually performing.

1 Introduction

Accelerated sea ice loss and the possibility of ice-free summers in the Arctic has increased the interest in potential human activities in the far North (Stephenson et al., 2011). To address the planning and safety concerns associated with this, government and private agencies need better predictions of sea-ice at sub-seasonal to seasonal time-scales (Jung et al., 2016). Over the past few years, many operational centers are already starting to provide such forecasts with longer lead times, although the skill of these forecasts – and how to assess the skill in the first place – is still under question (Smith et al., 2015).

There are numerous metrics to measure and quantify the accuracy of a forecast against observations, or ‘true’ conditions, depending on the variable in question (Wilks, 2019). Whether or not forecasts are considered skillful depends not only on the metric to measure the forecast error, but also what benchmark is used to measure skill against. The skill of the forecast produced by a particular forecast system can be compared against that of an earlier version of the same system (e.g., Balan-Sarojini et al., 2019), a different forecast

61 system (e.g., Zampieri et al., 2018, 2019), and also against a simpler reference forecast for
 62 benchmark (e.g., Woert et al., 2004; Pohlmann et al., 2004) .

63 Model outputs are commonly compared against two observation-based reference fore-
 64 casts: Climatology and Persistence. Climatology is based on the historical records for the
 65 given time of the year. An ensemble constructed from previous years can give a probabilistic
 66 estimate of the target variable. In the presence of a significant seasonal cycle and for lead
 67 times longer than just a few days, a climatological forecast needs to change with lead time
 68 according to the evolving time of the year. Persistence, on the other hand, is maintaining
 69 the initial state of the variable - thus giving a constant output of the variable. A persistence
 70 forecast can also be constructed such that the seasonal evolution, estimated from previous
 71 years, is taken into account, resulting in an anomaly persistence forecast. For either of these
 72 benchmark approaches, a secular trend can be taken into account to derive a trend-adjusted
 73 variant of such a forecast (Van den Dool et al., 2006). By design, persistence has better
 74 forecast skill at shorter lead times, whereas climatology is more skillful at longer lead times
 75 when errors approach a saturation level due to chaotic error growth (Woert et al., 2004).
 76 Finally, a damped anomaly persistence forecast attempts to combine persistence and clima-
 77 tology in such a way that it gradually transitions from the persisted to the climatological
 78 state, thereby optimizing the skill of the forecast at intermediate lead times (Van den Dool
 79 et al., 2006).

80 Anomaly persistence and damped anomaly persistence can be applied easily to contin-
 81 uous quantities on a grid-cell per grid-cell basis and have been used as benchmark forecasts
 82 for quantities such as sea-surface temperature on decadal timescale (e.g., Pohlmann et al.,
 83 2004) and sea-ice concentration on seasonal timescale (e.g., Blanchard-Wrigglesworth et al.,
 84 2011) . However, it is not trivial to transfer the concept of (damped) anomaly persistence
 85 to spatial objects such as the ice-edge location that corresponds to a binary, rather than
 86 a continuous, gridded field. For such a quantity, it can be difficult to establish meaningful
 87 autocorrelations at longer time scales; anomalies in this case tend to migrate spatially with
 88 the seasonal cycle (e.g., Goessling et al., 2016) , which means that initial anomalies at one
 89 location may not be relevant at the same location after some time, but they might still
 90 hold information about anomalies at a different nearby location. Properly utilising these
 91 anomalies for prediction thus requires consideration for how to transfer information across
 92 the domain and not just at increasing lead time.

93 In case of the ice edge, an important variable for marine activities in the Arctic, the
 94 mismatch between the predicted and ‘true’ ice edge can be quantified using the Spatial
 95 Probability Score (SPS; Goessling & Jung, 2018). The SPS (and its deterministic counter-
 96 part, the Integrated Ice Edge Error; see Goessling et al., 2016) determines the area where
 97 ice is either under-forecast or over-forecast in comparison to the true outcome. Palerme et
 98 al. (2019) compared the SPS to the (modified) Hausdorff distance (MHD; Dukhovskoy et
 99 al., 2015), another commonly used verification metric, and determined that the SPS is more
 100 robust and less affected by isolated patches of ice. Therefore, we will primarily be using SPS
 101 as the comparison metric in this paper, but will also use MHD to test whether our results
 102 are robust with respect to the choice of the metric.

103 In terms of lead-times, Zampieri et al. (2018, 2019) have shown that some operational
 104 subseasonal-to-seasonal (S2S) forecast systems are more skillful than climatology in predict-
 105 ing the location of the ice edge several weeks ahead. After 1.5 months, however, even the
 106 most skilful forecast system is not performing better than climatology. This can be compared
 107 against perfect-model studies that suggest that the ice-edge position can be predictable up
 108 to 6 months ahead (Goessling et al., 2016), suggesting that forecast calibration (not applied
 109 in Zampieri et al., 2018, 2019) and/or forecast system improvements should in principle
 110 be possible. Moreover, simple initial-state persistence tends to outperform these dynamical
 111 systems for at least the first 3-4 days, leaving a temporal window between about 4 to 45
 112 days where the best system can be considered skilful beyond the simple benchmark methods
 113 (Zampieri et al., 2018, 2019). However, given the simplicity of strict initial-state persistence

114 and climatology, the term skilful might be complacent in the sense that a less naive, but still
 115 simple, benchmark forecast method building on the concept of damped anomaly persistence
 116 may exhibit similar skill or even outperform existing dynamical forecast systems.

117 In this context, we have developed a method for predicting the location of the sea-
 118 ice edge that combines the climatologically derived probability of ice presence with initial
 119 (present) anomalies of the ice edge. Here we describe the method and an assessment of the
 120 forecasts produced. This paper is structured as follows: Data used for creating the forecasts
 121 are presented in section 2, followed by a description of the applied verification metrics
 122 in section 3. The Spatial Damped Anomaly Persistence (SDAP) method is described in
 123 detail in section 4. In section 5, we go through the results from verifying the forecasts
 124 produced with our method compared against other traditional references as well as against
 125 the performance of model-based S2S forecast systems. The paper concludes with a short
 126 discussion in section 6.

127 **2 Data**

128 **2.1 Sea-ice concentration observations**

129 We have used the Global Sea Ice Concentration Climate Data Record from OSI SAF
 130 to determine the climatological and initial sea-ice edge. The data is labelled as OSI-450 for
 131 years 1979 to 2015 and is based on satellite microwave measurements. From 2016 onwards,
 132 OSI-450 was extended as OSI-430b and is available with a 16 days latency. Alongside the
 133 microwave measurements, these products also use operational analyses and forecasts from
 134 ECMWF for atmospheric corrections. A near real time version of this record without the
 135 additional corrections is also available, as OSI-430. All of the data is freely available on the
 136 OSI SAF website and further details regarding the processing are described by Lavergne et
 137 al. (2019). OSI-450 (and OSI-430b) records are given on a Lambert Azimuthal Equal Area
 138 polar projection, also known as the EASE2 grid. The two hemispheres are separated and
 139 the horizontal grid spacing is 25km. Following this setup, our forecasts are also produced
 140 on the EASE2 grid at 25km resolution for each hemisphere.

141 **2.2 Subseasonal-to-seasonal (S2S) forecast data**

142 We compare the performance of our forecasts against the performance of the models
 143 from the Subseasonal to Seasonal (S2S) Prediction Project. The S2S database contains
 144 forecasts and reforecasts from several major operational centers. We have measured the
 145 concentration forecast of 5 dynamical sea ice forecasting system - the European Centre for
 146 Medium- Range Weather Forecasts (ECMWF), the Korea Meteorological Administration
 147 (KMA), Météo-France(MF), the National Centers for Environmental Prediction (NCEP),
 148 and the UK Met Office (UKMO). Alongside, we also used concentration forecasts from an
 149 older version of ECMWF (here named ‘ECMWFpres’) where the sea ice state is prescribed
 150 using initial persistence for the first 15 days and then relaxed toward climatology. Further
 151 description regarding the S2S project is given by Vitart et al. (2017). For a consistent
 152 comparison, all forecasts have been interpolated to a common grid with 1.5 degree horizontal
 153 resolution and only the period between 1999 and 2010 are considered in the analysis, in line
 154 with the analysis provided in Zampieri et al. (2018, 2019).

155 **3 Verification Metrics**

156 **3.1 Spatial Probability Score**

157 We are primarily using the Spatial Probability Score (SPS; Goessling & Jung, 2018)
 158 for verification of the sea-ice forecasts, which is defined as the spatial integral of the squared
 159 probability difference (i.e., the half-Brier Score). Since the S2S models provide ensemble
 160 forecasts of sea-ice concentration, we can derive a continuous (non-binary) probability of

ice-presence. The resulting score, which is in area units, quantifies the area of mismatch between forecast and observation. Measuring SPS of a deterministic, or binary, forecast results in the Integrated Ice Edge Error (IIEE; Goessling et al., 2016). We also use the SPS in our method for empirically optimising the weights by which our initial binary (anomaly persistence) forecast of the ice-edge location is damped towards climatology, resulting in a probabilistic (damped anomaly persistence) forecast, as detailed in Sect. 3.

3.2 Modified Hausdorff Distance

Given that we have used the SPS not only for evaluation but also for the empirical estimation of optimal damping weights (detailed below), we have also used a second verification metric to validate the skill of our method. The Modified Hausdorff Distance (MHD; Dukhovskoy et al., 2015; Palerme et al., 2019) measures the distance between two contours and the resulting score is in distance units. MHD can not consider non-binary probabilities, and therefore the probabilistic forecasts have been converted to a binary equivalent for measurement of MHD using the 50% contour of sea-ice probability. Since SPS and MHD measure forecast skill quite differently, using both metrics can reveal whether or not the forecasts from our method are skillful independent of the verification metric used.

4 Spatial Damped Anomaly Persistence (SDAP) Method

The steps towards creating the SDAP forecast of the ice-edge location can be divided into two parts. In the initialisation phase, the initial anomaly in ice-edge location is first derived from the climatological Sea Ice Probability (SIP; the probability of sea-ice concentration exceeding 15%) at points constituting the initially observed ice edge and then propagated (inherited) from the initial ice edge to each point of a (quasi-)global grid. In the forecasting phase, the inherited SIP and the climatology valid for the forecast target date are compared to determine first a deterministic ice-edge forecast by specifying “ice” versus “no ice” at each grid point, corresponding to an undamped anomaly persistence forecast, and second a probabilistic forecast by relaxing the deterministic forecast toward climatology, resulting in a damped anomaly persistence forecast.

Our method, detailed in the following, propagates the initial anomalies in local sea-ice extent in space by spatial inheritance, and then uses the spatial information to propagate the information in time based on the seasonal evolution of the climatological sea-ice probability. The rationale of this approach is based on the assumption that anomalies especially in the ice and ocean state associated with an ice-edge anomaly have a certain spatial and temporal correlation length. For example, if the ice edge extends further than usual into the ocean, this might have been caused thermodynamically by colder-than-usual regional temperatures (e.g., due to anomalous atmospheric circulation) that would also have caused thicker-than-usual and/or denser floes in the adjacent pack ice and colder-than-usual sea-surface temperatures (SST) in the adjacent open ocean. If this situation occurred during the melt season, the thicker-than-average ice would hamper the ice-edge retreat; if it occurred during the freeze season, the colder-than-average SST would facilitate the ice-edge advance.

4.1 Initialisation phase

For a given initial time, the fraction of years in the preceding 10 years with ice present (sea-ice concentration \geq 15%) at the same time of the year determines the raw climatological sea-ice probability (SIP) at each gridpoint. A larger number of years is not used in order to minimize the influence of long-term trends. The limited sample size however can result in spurious small-scale variations in the raw climatological SIP. Therefore a Gaussian filter with a radius of 220 km is applied to smooth the climatological probability field (exemplary result shown in figure 1). This results in smoother SIP contour lines which are advantageous for the subsequent steps of spatial inheritance.

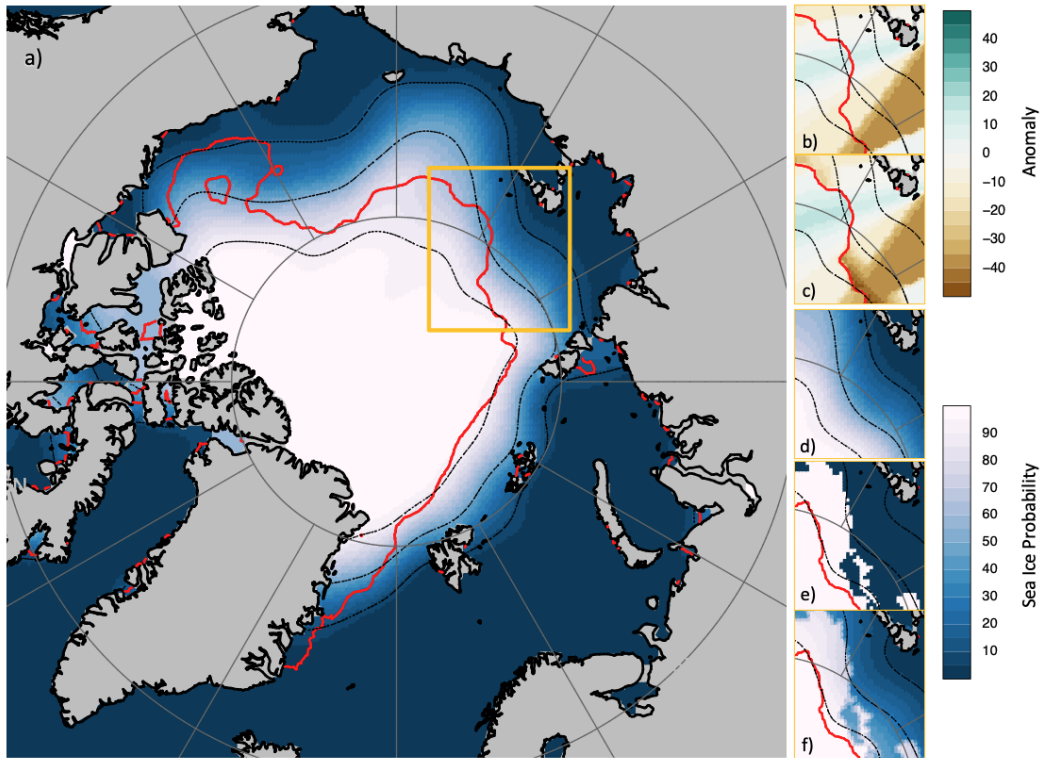


Figure 1. Map of the Arctic domain showing the climatological probability field for 1st of September 2020, and steps of the forecasting method (in insets) for the region selected. Insets ‘b’ and ‘c’ show the inherited and adjusted anomaly fields, ‘d’ shows the climatological probability field for the target date (30th of September, 2020), ‘e’ shows the Spatial Anomaly Persistence forecast and ‘f’ shows the Spatial Damped Anomaly Persistence forecast for the target date. In each panel, the red line denotes the 15% contour of the observed ice concentration for the relevant date while the dashed black lines show the 10%, 50% and 90% contour of the climatological probability field. Maps ‘b’ and ‘c’ use the Anomaly colour scale while all other maps use the Sea Ice Probability colour scale. Further details are in the text.

209 The initial ice edge, defined as the 15% contour of ice concentration on the initialisation
 210 date, is overlaid on the climatological probability. For every point along the contour, the
 211 climatological SIP at the nearest grid cell is used to compute the SIP anomaly in comparison
 212 to the median probability ($SIP = 50\%$) along the initial ice edge. If the ice edge is in a region
 213 of high (or low) climatological probability, the anomaly is negative (or positive). In other
 214 words, if the ice extent is higher than the median, the anomaly is positive and the ice edge
 215 should be in a region of low climatological probability. Next, this anomaly is mapped from
 216 the initial edge to the climatological median contour (corresponding to 50% ice-presence
 217 probability). This intermediate step has been introduced to avoid biased patterns of spatial
 218 inheritance that otherwise occur due to geometrical effects (not shown). The anomaly is
 219 then passed (spatially “inherited”) to the full grid using a nearest-neighbour match of the
 220 median contour from each grid cell, resulting in a map as shown in figure 1b.

221 In some cases, a grid cell with (without) ice in the initial observation might inherit
 222 a low (high) anomaly from the median, which causes the initial forecast at day 0 to not
 223 have (have) ice in the grid-cell. This initial mismatch generally occurs in cases where the
 224 observational gradient of ice presence is locally reversed compared to the climatological

225 gradient of ice presence probability. The problem is simply solved by checking the initial
 226 day forecast and replacing the anomaly inherited from the climatological median with the
 227 anomaly at the grid cell (i.e., the climatological probability of ice presence minus 50%) for
 228 grid cells with an initial mismatch. The result is a corrected probability anomaly map that
 229 can be persisted in time and used for forecasting.

230 4.2 Forecasting phase

231 Based on the corrected anomaly map from the initialisation phase (Fig. 1c), a forecast
 232 for any lead time can be created by simply adding the anomaly to the climatological SIP
 233 at each grid cell for the day in question. For example, if we initialise our forecast on
 234 September 1 and want to forecast the sea-ice edge 29 days later, then we add the anomaly
 235 from September 1 to the climatological SIP for September 30 (Fig. 1d). For every gridpoint,
 236 if the resulting probability is 50% or more, then we assign that point to be ice-present (as
 237 shown in inset ‘d’ of figure 1) . This gives a map of 1 (ice) and 0 (no-ice) which is our
 238 deterministic anomaly persistence forecast of ice-presence (Fig. 1e).

239 The binary anomaly persistence forecast, corresponding to a single sharp ice edge,
 240 does not take into account that the spatial and temporal correlation scales of anomalies
 241 are limited. For example, an initial ice-edge anomaly in March obviously carries much less
 242 information about ice-edge anomalies in the following September, when (in most Arctic
 243 regions) the ice edge will be far away from the initial location, and sufficient time will
 244 have passed to turn initial anomalies into largely uncorrelated anomalies. Therefore, we
 245 create a probabilistic ice forecast by damping our deterministic forecast towards climatology.
 246 For each lead-time, a damped probabilistic forecast is obtained as the weighted average of
 247 the deterministic prediction and the climatological probability. The optimal weights are
 248 determined by using a training set of forecasts, where we compute the SPS for anomaly
 249 weights between 0 and 1 in steps of 0.05, for each combination of lead time and initial time of
 250 the year, and find the weights minimising the error. The optimised anomaly weights (shown
 251 in section 3.3) can then be used for other, independent, years to get the probabilistic Spatial
 252 Damped Anomaly Persistence (SDAP) forecast (Fig 1 inset ‘f’). A schematic overview on
 253 the whole forecasting procedure is provided in Fig. S1.

254 In our study, we initialise the forecasts at the start of each month between 1989 and
 255 2020 and make predictions of the ice edge for the following year. The first 10 years of
 256 the period are used for empirical training to determine the anomaly weights and are thus
 257 excluded from the analysis. The remaining 22 years (1999 to 2020) have been used for
 258 the evaluation shown in the results below. For comparing to the forecasts from dynamical
 259 models in the S2S dataset (section 3.4), the forecasts from our method were interpolated
 260 to the coarse 1.5° S2S grid, and only years 1999 to 2010 were used, as in ZZampieri et al.
 261 (2018, 2019).

262 5 Results

263 Here, we present the evaluation of the forecasts from our method compared against
 264 other traditional benchmarks for ice-edge forecast, as well as against forecasts from dynamical
 265 models in the S2S dataset. Alongside climatological probability (hereafter referred to
 266 as CLIM) and initial-state persistence (PERS), the 50% contour of the climatological prob-
 267 ability has also been used to generate a binary forecast - the climatological median (CLIM-
 268 MED). Similarly, the 50% contour of the spatial damped anomaly persistence (SDAP) has
 269 been used to generate a median damped anomaly persistence forecast (SDAP-MED). Note
 270 that this is different from the binary Spatial Anomaly Persistence forecast (SAP) described
 271 above.

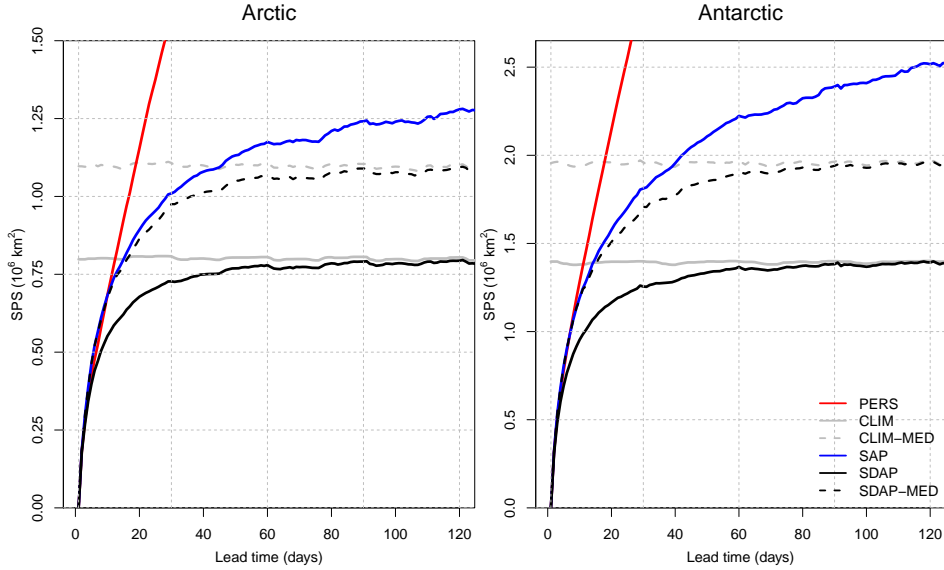


Figure 2. Spatial Probability Score (SPS) at increasing lead times (in days) for all forecasts averaged across all forecasts initialised between 1999 and 2020. The two dotted lines (CLIM-MED and SDAP-MED) are binary forecasts derived by assigning the ice edge at the 50% contour of the probabilistic forecasts (CLIM and SDAP). Further details are in the text.

5.1 Comparison against traditional benchmarks

The SPS result of all forecasts, averaged between 1999 and 2020 and across all seasons (Fig. 2), reveals that the performance of the SAP forecast is better than CLIM up to day 15 and better than CLIM-MED up to day 39 in both hemispheres. The performance of SDAP is better than SAP, outperforming CLIM at 2 months of lead time by an average of 0.03 million km² in the Arctic (0.04 million km² in the Antarctic). While SAP forecasts show an improvement over simple persistence from day 6, SDAP is better from day 3. The method design enables this forecast to perform at least as well as CLIM even at long lead times, leading it to be the most skillful forecast in this comparison set at all lead times except the first 2-3 days where PERS is marginally better.

Since the SPS considers the probabilistic information in a forecast, both CLIM and SDAP have a clear advantage over their binary counterparts. CLIM-MED has a near constant skill loss of 0.3 million km² in the Arctic (0.5 million km² in the Antarctic) compared to CLIM. The error of SDAP-MED is low initially (similar to the other anomaly forecasts) and converges towards the error of CLIM-MED, similar to how the error of SDAP converges towards the error of CLIM.

Given that our methodology uses the SPS to optimise damping weights, it is possible that using the SPS also as a verification metric leads to an overestimation of the skill. We thus also use the Modified Hausdorff Distance (MHD) as an independent verification metric, although the MDH can be applied only to the binary (median-based) forecast variants. While this verification method measures the forecast skill quite differently compared to SPS (Palermé et al., 2019), repeating the evaluation of the binary forecast variants with the MHD instead of the SPS provides overall a very similar picture: The SDAP-MED forecast outperforms the CLIM-MED forecast throughout the lead-time range, the undamped (SAP) forecast outperforms the CLIM-MED forecast up to 60 days lead time in the Arctic (43 days in the Antarctic), and simple persistence outperforms the other forecasts only slightly during

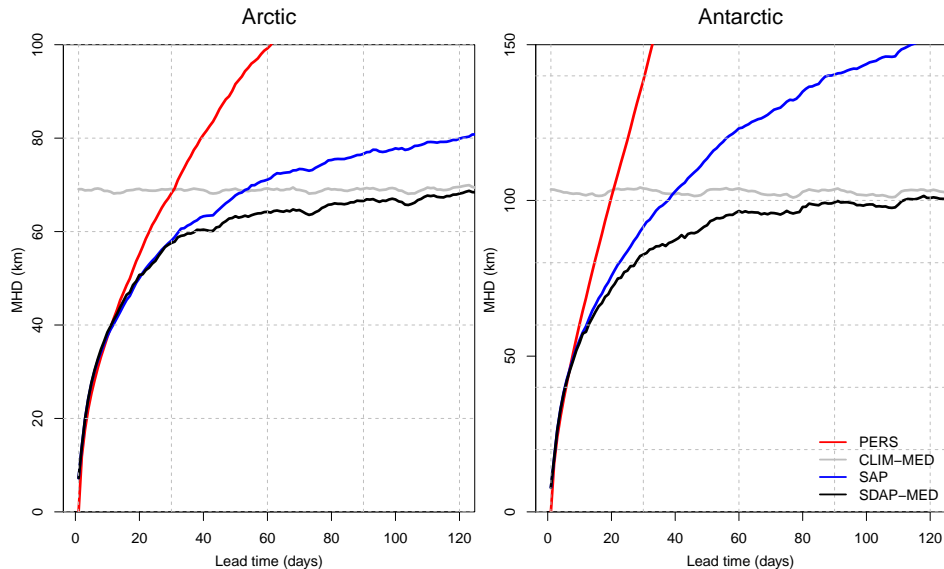


Figure 3. Same as figure 2, but for Modified Hausdorff Distance (MHD) of the binary forecasts compared to the observed ice edge.

298 the first few days (Fig. 4). The confirmation of the overall results with an independent metric
 299 provides additional confidence in our reference forecast method.

300 The previous analysis was based on outputs averaged over the entire time period. Given
 301 the strong seasonal cycle of Arctic sea ice and the processes that dominate the sea-ice budget,
 302 we now assess the performance of our method as a function of season. The forecast errors
 303 generally increase with lead time for all initialisation months, yet the actual score differs
 304 based on the month (Fig. 4). The errors are on average higher for the summer period in
 305 both hemispheres, and also during the late winter in the Arctic, when the sea ice is at its
 306 largest extent. These seasonal cycles can be linked to corresponding variations of the ice-
 307 edge length, although the December/January SPS maximum in the Antarctic is more likely
 308 related to enhanced interannual lateral ice-edge variability (Goessling et al., 2016).

309 For each initialisation month, the SDAP scores approach and then follow the SPS of
 310 climatology. Forecasts initialised in some months perform worse than climatology at long
 311 lead times, such as the Arctic forecasts initialised in June, despite the method design to
 312 merge the SDAP forecasts at long lead times to the climatological forecast. This is likely
 313 a result of sampling uncertainty and using different years for training the anomaly weights
 314 and for evaluating the forecast results, as detailed in the following.

315 5.2 Damping weights

316 As mentioned above, the deterministic anomaly forecasts are damped by empirically
 317 determined weights and added to an inversely weighted climatology to derive the proba-
 318 bilistic anomaly forecast. Here, the empirical fitting was done only over the optimisation
 319 period of 1989 to 1998 and a constant set of weights was then used for all forecasts within
 320 the evaluation period of 1999 to 2020. The weights, derived from the optimization period
 321 for each hemisphere separately (Fig. 4), reveal the timescale at which information from the
 322 initial anomalies is lost and climatology becomes more informative. By day 30, the initial-
 323 anomaly weights decrease to 50% for most initialisations, but most forecasts have not been
 324 completely damped to climatology even at 3 months of lead time. In both hemispheres,

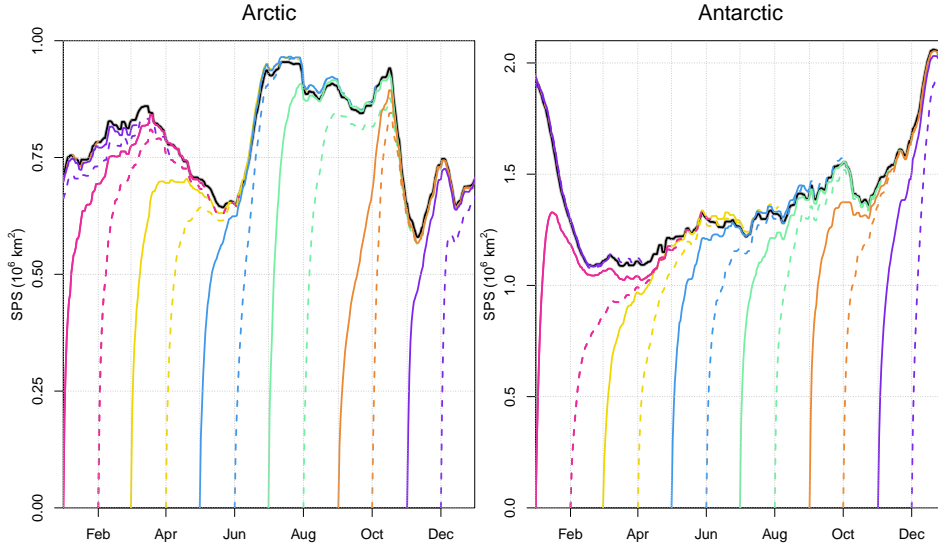


Figure 4. SPS for the first 120 days of SDAP forecasts initialised at the start of each month (as represented by the coloured lines), alongside CLIM for each date (black continuous line), with results averaged between 1999 and 2020.

325 the anomaly weight stays high for a longer period at the end of the summer melt season -
 326 August/September in the Arctic and February in the Antarctic.

327 The weight of the anomaly is not always decreasing monotonically (see figure 5), al-
 328 though in general the influence of initial conditions should decrease with time. While some
 329 intermittent fluctuations can be caused by sampling uncertainty due to the limited optimi-
 330 sation period, we argue that some of this can be linked to what is known as reemergence
 331 of sea-ice anomalies (Blanchard-Wrigglesworth et al., 2011): When over the course of the
 332 seasonal cycle the (climatological) ice edge first migrates away from the initial location and
 333 then returns to a similar location later, the initial ice-edge anomalies may carry more in-
 334 formation for that later state than for the earlier - but more remote - intermediate state.
 335 This seems to be the case in particular for the Arctic forecasts initialised at the beginning
 336 of August, which exhibit a local minimum of the anomaly weight around day 35-40 (around
 337 the sea-ice minimum) and higher weights again thereafter until around day 70 (Fig. 5).
 338 The increased anomaly weight acts to keep the associated forecast error below the error of
 339 climatology for longer compared to other initialisation months (Fig. 4).

340 5.3 September 2020 as an illustrative example

341 To illustrate our forecast method, we now consider the example of the Arctic ice edge
 342 with the initial condition on the 1st of September, 2020, as shown in Fig. 1. Sea-ice extent in
 343 the Arctic during September 2020 was the second lowest in satellite records and during Oc-
 344 tober 2020 was the lowest October ice extent measured ((NSIDC, 2020). Persistent offshore
 345 winds from the Siberian coast, associated with a positive phase of the Arctic Oscillation
 346 (AO) during the preceding winter, meant that the Eurasian parts of the Arctic were mostly
 347 ice-free and had strong negative anomalies (as seen in Fig. 1b).

348 SDAP forecasts in this particular case are better in the American part of the Arctic than
 349 in the Eurasian part. The forecasts correctly suggest that positive anomalies would persist in

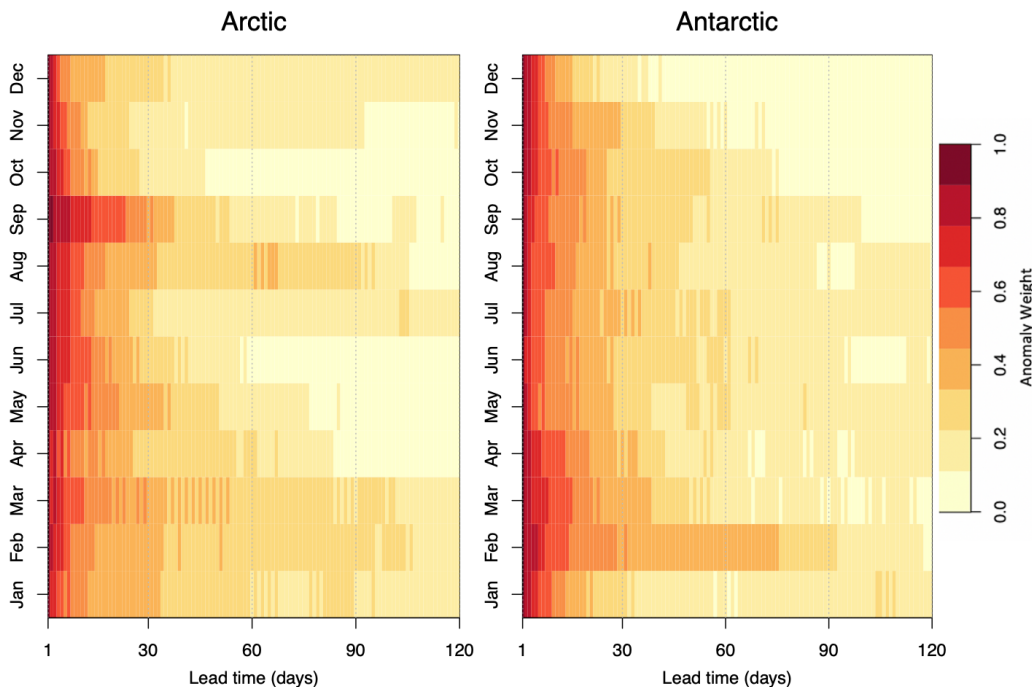


Figure 5. Anomaly weights for the SDAP forecast as a function of initialisation month and lead time (first 120 days). These weights determine the ratio of SAP forecast to climatology in the SDAP forecast and are measured using optimization of SPS as described in the text.

350 the southeastern Beaufort Sea (on the left in each panel of Fig. 6) until the end of the month,
 351 and even the persistence of the ice-free patch within the ice cover of the Beaufort Sea is
 352 correctly forecast, although the position is shifted. In the Greenland Sea and Fram strait, the
 353 forecasts are fairly accurate at day 15 and 30, and still better than the climatological median
 354 at day 45. North of the Laptev Sea, the forecast retains the initial negative anomalies - as
 355 dictated by the concept of anomaly persistence - and thus shows a similarity in shape to the
 356 initial ice edge. While a small patch remains accurately ice-free at day 30, the overall forecast
 357 in this region shows an expansion of the high-probability areas toward the coast following
 358 the seasonal evolution of the climatological probabilities. By contrast, the actual ice edge
 359 does not follow the usual seasonality but remains largely unchanged, thereby developing
 360 even stronger negative anomalies. The SDAP forecast remains better than climatology, but
 361 the anomaly intensification is not captured. This highlights the limitation of the SDAP
 362 approach, given that it is based on the persistence of anomalies.

363 North of Franz Joseph Land, the initial anomaly is strongly negative, yet there is ice
 364 present along the island coasts (in a positive anomaly region), allowing some parts of the
 365 median edge to inherit positive anomalies. Depending on the exact position of a grid cell
 366 in relation to the median and ice-edge contours, it might inherit slightly different anomalies
 367 and predict different ice conditions. This can be seen in the SDAP forecast for day 45, where
 368 some grid cells of the ocean in this region have a lower probability of ice-presence than the
 369 surrounding region. We discuss this issue further in section 6.

370 5.4 Comparison against S2S dataset

371 The main motivation for this study is to use the damped anomaly forecast as a reference
 372 benchmark for evaluating dynamical sea-ice models. Therefore, here we compare the per-
 373 formance of the forecasts from this method against those from the S2S Prediction database

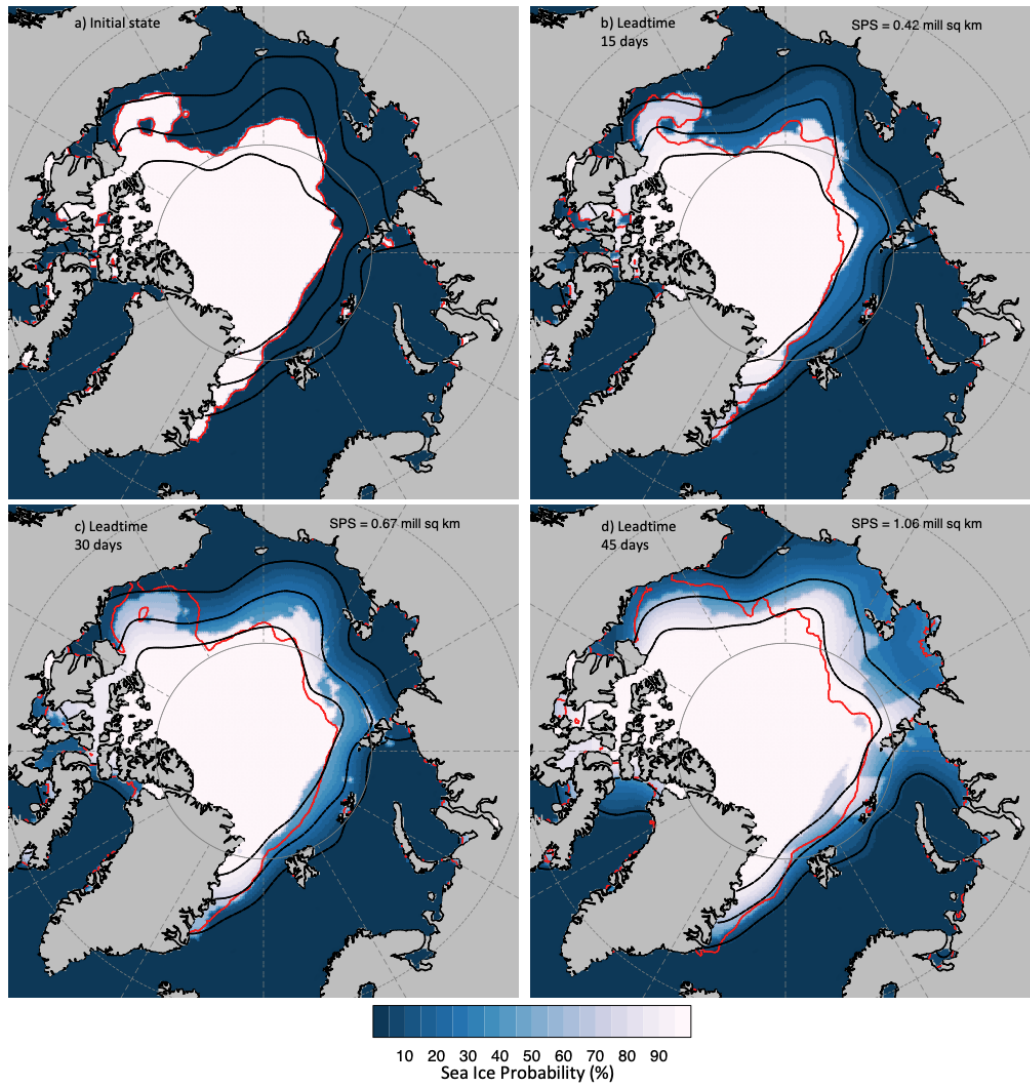


Figure 6. Observed sea ice conditions in the Arctic for 1st of September, 2020 and the corresponding SDAP forecasts at lead times of 15, 30 and 45 days. In each of the panels, the green lines show the contours of climatological probability (10, 50 and 90%), while the red line shows the actual ice edge on the respective date.

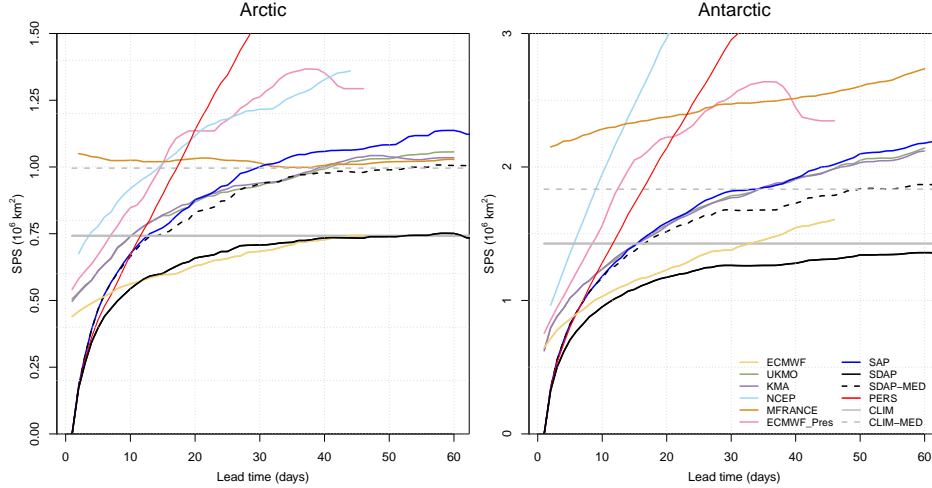


Figure 7. SPS for forecasts from the S2S dataset, alongside climatology (CLIM), initial state persistence (PERS), Spatial Anomaly Persistence (SAP) and Spatial Anomaly Damped Persistence (SDAP) forecasts, averaged across all seasons and years between 1999 and 2010.

374 (Vitart et al., 2017), in line with the analyses presented in Zampieri et al. (2018, 2019). The
 375 results for the S2S models shown here are similar to those found by Zampieri et al. (2018,
 376 2019), although the scores have increased throughout due to the use of a larger sea-mask.
 377 The SDAP forecasts for years 1999 to 2010 were remapped to the common 1.5° S2S grid
 378 for this analysis and this has led to an increase in forecast error relative to climatology - in
 379 contrast to the evaluation on the OSI-SAF grid (Fig. 2), the SDAP error now reaches and
 380 slightly surpasses the climatological error around 60 days lead time in the Arctic (Fig. 7 left;
 381 see also Fig. S3).

382 The undamped (thus binary) SAP forecast has a similar forecast skill as UKMO and
 383 KMA in both hemispheres (Fig. 7), despite the fact that these forecast systems have the
 384 advantage of providing ensemble-based probabilities rather than a binary ice edge. The
 385 damped (thus probabilistic) SDAP forecast in the Arctic clearly outperforms UKMO and
 386 KMA and is about as skillful as ECMWF. The latter is the best-performing model in the
 387 S2S set (Zampieri et al., 2018, 2019) and (without calibration) the only one that is more
 388 skillful than climatology beyond day 15 in the annual average. In the Antarctic, our SDAP
 389 method even outperforms the ECMWF ensemble, in particular beyond 20 days lead time
 390 when the ECMWF system appears to develop biases so that climatology provides a better
 391 forecast beyond 32 days lead time.

392 To assess the robustness of our results and to avoid a skill overestimation for our bench-
 393 mark method due to the use of the SPS for the weight optimisation, we now compare the
 394 performance of the SDAP forecasts against those from the S2S dataset using Modified Haus-
 395 dorff Distance (MHD; Fig. S2). Due to the differences in the method, including that MHD
 396 can be applied only to binary forecasts (based on the median ice edge where applicable),
 397 MHD measurements do not precisely mirror the results of the SPS measurements (for all
 398 models). Yet the ranking of the models is similar. The anomaly forecasts have a high skill
 399 compared to most other models or climatology. The average MHD of the ECMWF forecasts
 400 is again the lowest in the S2S set, except at short lead times below 12 days. The SDAP
 401 forecasts outperform the ECMWF forecasts in the short range and roughly match the skill
 402 of ECMWF at longer lead times, particularly in the Antarctic.

6 Summary and Conclusion

This paper describes a novel method for forecasting the presence and extent of ice in the Arctic or Antarctic based on persistence and damped persistence of probabilistic anomalies. The method requires only historical and initial ice-presence information to make the predictions, yet remains more skillful than climatological forecasts at month-long lead times. This is in contrast to most of the models from the S2S database, of which (without calibration) only one model performs better than climatology beyond 12 days of lead time.

The SDAP method uses the probabilistic anomaly from the initial date, which is spatially distributed (“inherited”) by a nearest-neighbour search, and adds it to the climatology of the target date to generate a deterministic anomaly persistence forecast. With increasing lead time the probabilistic anomaly is damped to generate a probabilistic forecast. At longer lead times, one can expect that dynamical and thermodynamical processes cause the initial anomalies to be less informative. Therefore, the method has been designed to increase the damping with time and converge to climatology at long lead times. The damping weights, determined empirically using the reforecasts between 1989 and 1998, show that initial anomalies remain highly informative (weight $> 30\%$) for about 20-30 days in most months, and even longer in late summer. It is possible that in the Arctic, as the climatological ice-edge shifts with the continued decrease in ice extent, the optimal damping weights might also change.

We note that there are instances of sharp spatial transitions in the anomalies inherited to the grid (as described in section 5.3) due to the spatial distribution of the initial ice edge. Spatially smoothing the anomaly before passing it to the grid could smoothen the transition. Explicitly adding a spatial component to the damping might also be better than using a pan-Arctic damping weight evolving only with lead time. This might also have the potential to implicitly capture the re-emergence of anomalies when the ice edge returns to a location over the course of the seasonal cycle after the extent has reached its maximum or minimum. Nevertheless, the empirical approach used here, while simplistic, gives a good estimation of the overall decrease in the information content of the anomalies.

While our results show that the damped anomaly forecast outperforms most of the models in the S2S dataset, it must be noted that the skill of the dynamical sea-ice models could be higher than shown after bias correction or other forms of forecast calibration, which is standard for forecasts of other predictands at subseasonal-to-seasonal timescales. Forecast calibration remains challenging for sea ice, although promising approaches have recently been suggested (e.g., Dirkson et al., 2019; Director et al., 2017). Moreover, the resolution of the common S2S grid is low, and forecast skill was found to deteriorate after interpolation into this grid (Fig S3). It is possible that measuring the performance of the S2S models on their native grid would have resulted in a higher skill. The models output several variables, whereas our method is designed to only forecast ice-presence. Combining these outputs, or simply using a different concentration threshold, could also lead to more skill in the predictions, as shown by Zampieri et al. (2019).

The SDAP method, applied here for predicting ice-presence equivalent to 15% or more sea-ice concentration, could also be used for predicting other binary fields. Considering sea-ice concentration, Mizuta et al. (2008) proposed a different probabilistic method to estimate ice concentration by combining individual predictions for different concentration thresholds; While the method is quite different, a similar framework for our method can be used for estimating ice concentration or thickness by using several binary levels. Furthermore, the damped anomaly prediction method might also have applications in other fields not related to sea ice.

To conclude, the method proposed here is on average as skillful as the ECMWF forecast system, which is the most skillful one in the S2S database. Comparing only against persistence and climatology can give the impression that sea-ice forecasts from some of the

454 S2S forecast systems can already be regarded as “skillful” and thus of potential value for
 455 users. However, using a more challenging benchmark such as the spatial damped anomaly
 456 persistence (SDAP) method introduced here reveals that the forecast systems still have a
 457 way to go until they can generate substantial value beyond much simpler methods. We
 458 hope that, by including more challenging benchmark forecast methods such as ours in their
 459 evaluation workflow, other researchers and forecasting centers can build a better basis to
 460 improve their sea-ice forecast systems.

461 Acknowledgments

462 All data analyzed here are openly available. The OSI-SAF sea ice concentration product can
 463 be retrieved from the MET Norway FTP server at <ftp://osisaf.met.no/reprocessed/ice/>. The
 464 S2S forecasts data can be retrieved from the ECMWF data portal at <http://apps.ecmwf.int/datasets/data/s2s/levtype=sfc/type=cf/>. We are grateful to the World Weather Research
 465 Program (WWRP) and to the World Climate Research Program (WCRP), to operational
 466 forecast centers and individuals that contributed to the S2S database, as we are grateful
 467 to all those involved in implementing and maintaining the database. We acknowledge the
 468 OSI-SAF consortium for making their sea ice concentration products available. A special
 469 thanks to Lorenzo Zampieri and Barbara Casati for providing helpful comments and dis-
 470 cussions regarding our work. This paper is a contribution to the Year of Polar Prediction
 471 (YOPP), a flagship activity of the Polar Prediction Project (PPP), initiated by the World
 472 Weather Research Programme (WWRP) of the World Meteorological Organisation (WMO).
 473 We acknowledge the WMO WWRP for its role in coordinating this international research
 474 activity. We acknowledge the financial support by the Federal Ministry of Education and
 475 Research of Germany in the framework of SSIP (grant 01LN1701A).
 476

477 References

- 478 Balan-Sarajini, B., Tietsche, S., Mayer, M., Alonso-Balmaseda, M., & Zuo, H. (2019).
 479 *Towards improved sea ice initialization and forecasting with the ifs*. Retrieved 2021-
 480 07-01, from [https://www.ecmwf.int/en/e-library/18918-towards-improved-sea-](https://www.ecmwf.int/en/e-library/18918-towards-improved-sea-ice-initialization-and-forecasting-ifs)
 481 [ice-initialization-and-forecasting-ifs](https://www.ecmwf.int/en/e-library/18918-towards-improved-sea-ice-initialization-and-forecasting-ifs)
- 482 Blanchard-Wrigglesworth, E., Bitz, C. M., & Holland, M. M. (2011, 09). Influence of
 483 initial conditions and climate forcing on predicting arctic sea ice. *Geophysical Research*
 484 *Letters*, *38*, n/a-n/a. doi: 10.1029/2011gl048807
- 485 Director, H. M., Raftery, A. E., & Bitz, C. M. (2017, 12). Improved sea ice forecasting
 486 through spatiotemporal bias correction. *Journal of Climate*, *30*, 9493-9510. doi:
 487 10.1175/jcli-d-17-0185.1
- 488 Dirkson, A., Merryfield, W. J., & Monahan, A. H. (2019, 02). Calibrated probabilistic
 489 forecasts of arctic sea ice concentration. *Journal of Climate*, *32*, 1251-1271. doi:
 490 10.1175/jcli-d-18-0224.1
- 491 Dukhovskoy, D. S., Ubnoske, J., Blanchard-Wrigglesworth, E., Hiester, H. R., & Proshutin-
 492 sky, A. (2015, 09). Skill metrics for evaluation and comparison of sea ice models. *Jour-*
 493 *nal of Geophysical Research: Oceans*, *120*, 5910-5931. doi: 10.1002/2015jc010989
- 494 Goessling, H. F., & Jung, T. (2018, 04). A probabilistic verification score for contours:
 495 Methodology and application to arctic ice-edge forecasts. *Quarterly Journal of the*
 496 *Royal Meteorological Society*, *144*, 735-743. doi: 10.1002/qj.3242
- 497 Goessling, H. F., Tietsche, S., Day, J. J., Hawkins, E., & Jung, T. (2016, 02). Predictability
 498 of the arctic sea ice edge. *Geophysical Research Letters*, *43*, 1642-1650. doi: 10.1002/
 499 2015gl067232
- 500 Jung, T., Gordon, N. D., Bauer, P., Bromwich, D. H., Chevallier, M., Day, J. J., ... Yang,
 501 Q. (2016, 09). Advancing polar prediction capabilities on daily to seasonal time
 502 scales. *Bulletin of the American Meteorological Society*, *97*, 1631-1647. doi: 10.1175/
 503 bams-d-14-00246.1
- 504 Lavergne, T., Sørensen, A. M., Kern, S., Tonboe, R., Notz, D., Aaboe, S., ... Pedersen,

- 505 L. T. (2019, 01). Version 2 of the eumetsat osi saf and esa cci sea-ice concentration
 506 climate data records. *The Cryosphere*, *13*, 49-78. doi: 10.5194/tc-13-49-2019
- 507 Mizuta, R., Adachi, Y., & Kusunoki, S. (2008). *Estimation of the future distribution of sea*
 508 *surface temperature and sea ice using the cmip3 multi-model ensemble mean*. Retrieved
 509 2020-07-01, from [https://www.mri-jma.go.jp/Publish/Technical/DATA/VOL_56/](https://www.mri-jma.go.jp/Publish/Technical/DATA/VOL_56/tec_rep_mri_56.pdf)
 510 [tec_rep_mri_56.pdf](https://www.mri-jma.go.jp/Publish/Technical/DATA/VOL_56/tec_rep_mri_56.pdf)
- 511 NSIDC. (2020, 10). *October — 2020 — arctic sea ice news and analysis*. Retrieved 2021-
 512 01-01, from <https://nsidc.org/arcticseaicenews/2020/10/>
- 513 Palerme, C., Müller, M., & Melsom, A. (2019, 05). An intercomparison of verification scores
 514 for evaluating the sea ice edge position in seasonal forecasts. *Geophysical Research*
 515 *Letters*, *46*, 4757-4763. doi: 10.1029/2019gl082482
- 516 Pohlmann, H., Botzet, M., Latif, M., Roesch, A., Wild, M., & Tschuck, P. (2004, 11).
 517 Estimating the decadal predictability of a coupled aogcm. *Journal of Climate*, *17*,
 518 4463-4472. doi: 10.1175/3209.1
- 519 Smith, G. C., Roy, F., Reszka, M., Surcel Colan, D., He, Z., Deacu, D., ... Lajoie, M.
 520 (2015, 05). Sea ice forecast verification in the canadian global ice ocean prediction
 521 system. *Quarterly Journal of the Royal Meteorological Society*, *142*, 659-671. doi:
 522 10.1002/qj.2555
- 523 Stephenson, S. R., Smith, L. C., & Agnew, J. A. (2011, 05). Divergent long-term trajectories
 524 of human access to the arctic. *Nature Climate Change*, *1*, 156-160. doi: 10.1038/
 525 nclimate1120
- 526 Van den Dool, H. M., Peng, P., Johansson, A., Chelliah, M., Shabbar, A., & Saha, S. (2006,
 527 12). Seasonal-to-decadal predictability and prediction of north american climate—the
 528 atlantic influence. *Journal of Climate*, *19*, 6005-6024. doi: 10.1175/jcli3942.1
- 529 Vitart, F., Ardilouze, C., Bonet, A., Brookshaw, A., Chen, M., Codorean, C., ... Zhang, L.
 530 (2017, 01). The subseasonal to seasonal (s2s) prediction project database. *Bulletin of*
 531 *the American Meteorological Society*, *98*, 163-173. doi: 10.1175/bams-d-16-0017.1
- 532 Wilks, D. S. (2019). Forecast verification. *Statistical Methods in the Atmospheric Sciences*,
 533 369-483. doi: 10.1016/b978-0-12-815823-4.00009-2
- 534 Woert, M. L. V., Zou, C.-Z., Meier, W. N., Hovey, P. D., Preller, R. H., & Posey,
 535 P. G. (2004, 06). Forecast verification of the polar ice prediction system
 536 (pips) sea ice concentration fields. *Journal of Atmospheric and Oceanic Technol-*
 537 *ogy*, *21*, 944-957. Retrieved 2021-07-01, from [https://journals.ametsoc.org/](https://journals.ametsoc.org/view/journals/atot/21/6/1520-0426_2004_021_0944_fvotpi_2.0_co_2.xml)
 538 [view/journals/atot/21/6/1520-0426_2004_021_0944_fvotpi_2.0_co_2.xml](https://journals.ametsoc.org/view/journals/atot/21/6/1520-0426_2004_021_0944_fvotpi_2.0_co_2.xml) doi:
 539 10.1175/1520-0426(2004)021<0944:FVOTPI>2.0.CO;2
- 540 Zampieri, L., Goessling, H. F., & Jung, T. (2018, 09). Bright prospects for arctic sea ice
 541 prediction on subseasonal time scales. *Geophysical Research Letters*, *45*, 9731-9738.
 542 doi: 10.1029/2018gl079394
- 543 Zampieri, L., Goessling, H. F., & Jung, T. (2019, 08). Predictability of antarctic sea ice
 544 edge on subseasonal time scales. *Geophysical Research Letters*, *46*, 9719-9727. doi:
 545 10.1029/2019gl084096

Challenging Dynamical Forecast Systems with Spatial Damped Anomaly Persistence for the Sea-Ice Edge

Bimochan Niraula, Helge F. Goessling

Alfred-Wegener-Institut Helmholtz-Zentrum für Polar- und Meeresforschung

Contents of this file

Figures S1 to S3

Introduction

This file contains three figures. The first figure shows a schematic showing the steps taken in deriving the Spatial Damped Anomaly Forecast from initial and climatological sea-ice concentration data. The second figure is the result of the average Modified Hausdorff Distance (MHD) for forecasts from the S2S database, as well as the traditional reference and anomaly forecasts. The third figure shows the change in mean SPS for CLIM and SDAP forecast after interpolation into the common S2S grid and after applying the common mask. Each figure has an attached caption with additional information.

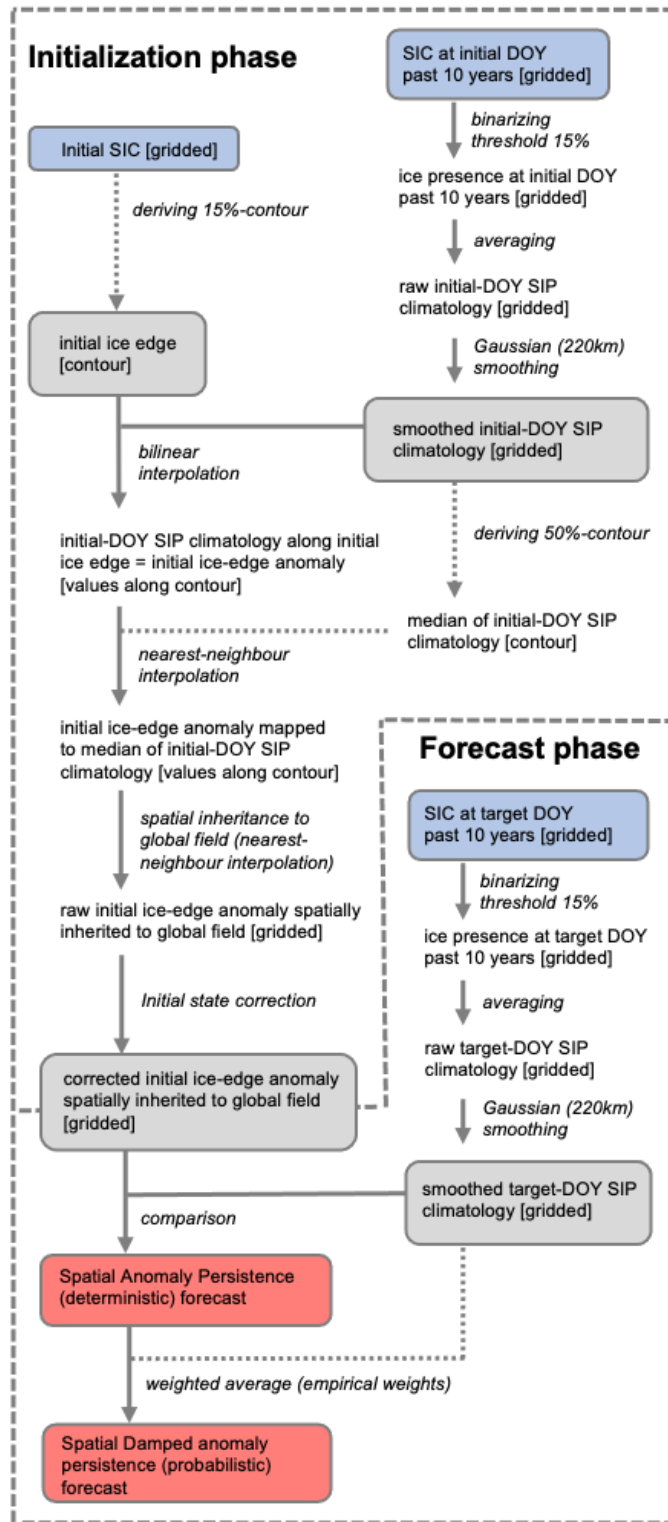


Figure S1. Schematic of the Spatial Damped Anomaly Persistence method as described in the main publication. The only data used as input for the method is SIC at initial date and climatological SIC, found using the SIC for the same DOY for the past 10 years. Further information is in the main text.

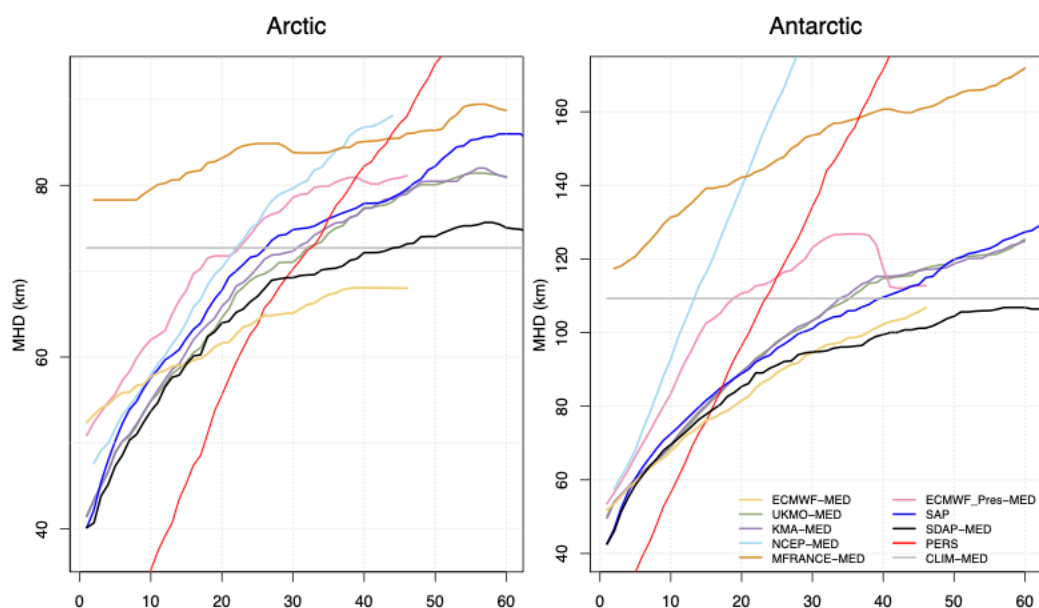


Figure S2. Same as figure 7, but for Modified Hausdorff Distance (MHD), using the 50% probability threshold to create the binary forecasts. For the probabilistic forecasts, the median probability of ice presence is used to determine the predicted ice edge. Due to the resolution of the S2S grid and the disconnected segments of the ice-edge, the MHD measurements do not precisely mirror the results of the SPS measurements. Nevertheless, the ranking of the models is similar to that found using SPS and we can confirm that the SDAP forecasts perform better than all models in the S2S database except ECMWF.

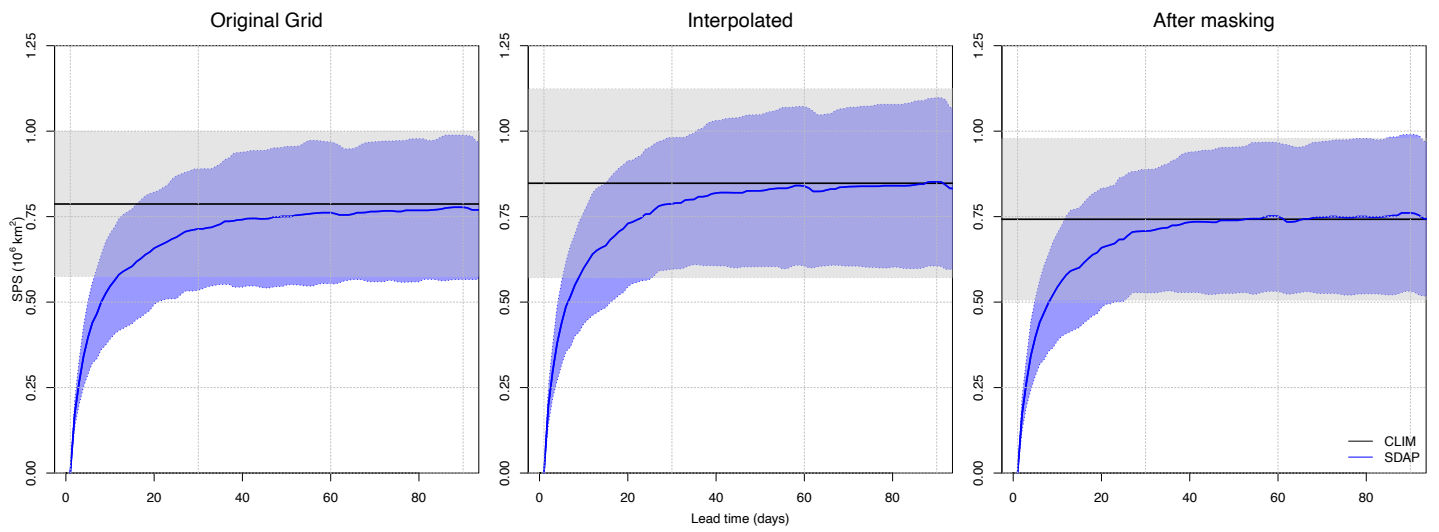


Figure S3. A comparison between the SPS of climatological forecast (CLIM) and the Spatial Damped Anomaly Persistence forecast (SDAP) in the original grid, after interpolation to the common S2S grid and after applying a common mask. The mask is derived by finding all grid-cells, where each of the forecast systems being compared has either ice or ocean. Results show the average of all forecasts for years 1999 to 2010, while the shaded areas show +/- 1 standard deviation.